Sl. No.	IIT Ropar List of Recent Publications with Abstract Coverage: October, 2020
1.	A Method for Surface Voltage Measurement of an Overhead Insulated Conductor AJ Thomas, C Iyyappan, CC Reddy - IEEE Transactions on Instrumentation and Measurement, 2020 **Abstract:** Surface voltage measurement of an insulated overhead conductor assumes importance for understanding corona, radio interference voltage and for design purposes. Surface voltage measurement of a bare overhead conductor is quite simple as a voltage divider can be directly connected. However, there are challenges in the measurement of surface voltage on an insulating surface of an insulated covered conductor using voltage dividers. In case of ac measurements, the capacitance parameter dominates in deciding the potential distribution. In this paper, it is demonstrated that the measuring system itself will alter the voltage division between the capacitance of the cylindrical insulated conductor and that of surrounding air acting as a capacitive divider. The voltage distribution is shown to be drastically influenced by the measuring system capacitance. In view of these issues, a novel experimental method is proposed for the measurement of surface voltage of an overhead insulated covered conductor. In general, the method can be applied to any cylindrical insulated conductor and for calibration of sensor based measurements. The proposed empirical method is tested by a validated simulation of the entire system and it is proven analytically. The radial voltage gradients are then estimated from measured surface voltages. The analytical, experimental and simulation results are in close conformity.
2.	A systematic experimental study of pre-compound emission in αα-particle induced reactions on odd mass nuclei A = 103–123 MK Sharma, M Kumar, M Shuaib, I Majeed, MS Asnain…PP Singh.. - The European Physical Journal A, 2020 **Abstract:** The compound and pre-compound emission processes have been established as two main competing de-excitation modes of an excited nucleus by-dint-of evaporation and emission of light fast particles in low energy αα-induced reactions, respectively. An existence of the plenty experimental data on above established processes for a wide range of mass nuclei coerces to drive for some systematic trends in such reactions with excitation energy and mass number (A). Present work is an attempt to develop a systematics on the pre-compound emission process by analysing consistent experimental cross-section data of αα-particle induced reactions on odd Z and odd A isotopic target nuclei viz., 103103Rh, 107107Ag, 109109Ag, 113113In, 115115In, 121121Sb, and 123123Sb, respectively. The analysis of data indicates sarcastic deviation in the experimental cross-section data with respect to calculations performed by the statistical Monte-Carlo code PACE4 beyond the peak region. Such deviation becomes more prominent towards tail portion of excitation functions, which is regarded as a significant contribution of the pre-compound emission process. Observed energy dependent uniformity of such deviation for all studied reactions gives a clue for existing some systematics on concerning process with atomic mass number (A). Present study is an extension of previous work [Eur. Phys. J. A 54, 205 (2018)], but rather in more precise way for nearby isotopic target mass nuclei 107107Ag, 109109Ag, 113113In, 115115In, 121121Sb, and 123123Sb, respectively, where role of the Coulomb barrier Vbb and target deformation is found to be significantly important in the systematic decay of excited nuclei through emission of light fast particles in pre-compound process with mass number (A).

3.	An Account of the Catalytic Transfer Hydrogenation and Hydrogenolysis of Carbohydrates-Derived Renewable Platform Chemicals over Non-Precious Heterogeneous Metal Catalysts R Srivastava, A Shivhare, A Kumar – ChemCatChem, 2020 **Abstract:** Sustainable and eco-friendly catalytic processes for renewable lignocellulose biomass conversion into liquid fuels and useful chemicals offer solutions to minimize greenhouse gases emission and associated negative climate impacts. Lignocellulose derived cellulose and hemicellulose can be converted into platform chemicals including glucose, fructose, xylose, hydroxymethylfurfural, furfural, levulinic acid, levulinate esters, etc. These platform chemicals can be subsequently converted into liquid fuels and value-added chemicals using heterogeneous catalytic processes such as; oxidation, hydrogenation, hydrogenolysis, etc. The catalytic transfer hydrogenation and hydrogenolysis (CTH) over non-precious metal catalysts have recently drawn considerable research interest. This review summarizes recent progress on non-precious metals catalyzed CTH processes, which also include photocatalysis and electrocatalysis, for the transformation of 5-hydroxymethylfurfural, furfural, levulinic acid, and, levulinate esters into furfuryl alcohol, 2-methylfuran, 2,5-dimethylfuran, and, gamma-valerolactone; elucidate structure-function relationship and highlights the underlying reaction mechanisms. This review is timely and provides detailed fundamental insights about the nature of active sites and CTH processes that will be useful for the researchers willing to work in this exciting area.
4.	An Optimal Architectural Design for Unconventional Modular Reconfigurable Manipulation System A Dogra, SS Padhee, E Singla - Journal of Mechanical Design, 2020 **Abstract:** Modular and Reconfigurable manipulators have gained popularity especially in the service sector, where the use of customized configurations has increased. Adaptable modular designs have come into advances in achieving the required configuration of a robotic manipulator. As reported in the literature, various designs of the modules mainly with conventional configurations are presented and a few are reported with unconventional adjustments. To cater the non-repetitive applications, this paper presents an optimal architectural design for unconventional parameters for customized reconfigurability. This lighter and easier to connect version is also applicable to n-DoF and unconventional robotic parameters. Architecture Prominent Sectioning (APS) strategy is proposed which assumes an architecture as a set of point masses and optimally relocate components with respect to the minimization of the joint torques. Modules are considered to be 3-D printables using poly-lactic acid (PLA), a thermoplastic material, and thus light in weight. The new modular architecture design is validated through the assemblage of conventional/unconventional configurations using two types of modules namely Heavy(H) and Light(L). Along with that, worst torque analysis for the different configurations has been done in order to provide a strategy for assembly combinations. A comparative study is presented based upon the payload to the manipulator weight ratio, involving other reported architectures.
5.	Assessing the Impact of COVID-19 on Interactions among Stock, Gold and Oil Prices in India P Mukherjee, S Bardhan - Trade and Development Review, 2020 **Abstract:** This paper attempts to explore the relationship between the stock prices and the prices of two mostly traded commodities in the derivatives market, viz. crude oil and gold in the Indian context. Based on the daily data during 2017-2020, the paper employs ARDL model in order to estimate the long-term relationships. It also finds out the impact of market disruptions following

	the recent COVID-19 pandemic, on this relationship in the context of Indian financial markets. The findings point to the fact that the stock returns and the commodity prices are closely linked with each other. Interestingly, our findings suggest that the pandemic has altered the relationship. In the pre-COVID period, there was no cointegration among the stock, gold and crude oil prices. However, during the pandemic, we find evidence of cointegrating relationships. The short run relationship also provides some interesting insights. In the pre-pandemic period, evidence points to a mutual impact on the two markets, e.g. past values of oil price and gold price influence the stock returns while returns on the stock market influences oil price volatility. However, during the COVID period, apart from crude oil prices, it is the volatility of gold prices that has emerged as the driver of the stock returns.
6.	Background magnetic field and quantum correlations in the Schwinger effect S Bhattacharya, S Chakrabortty, H Hoshino, S Kaushal - Physics Letters B, 2020 **Abstract:** In this work we consider two complex scalar fields distinguished by their masses coupled to constant background electric and magnetic fields in the (3+1)-dimensional Minkowski spacetime and subsequently investigate a few measures quantifying the quantum correlations between the created particle-antiparticle Schwinger pairs. Since the background magnetic field itself cannot cause the decay of the Minkowski vacuum, our chief motivation here is to investigate the interplay between the effects due to the electric and magnetic fields. We start by computing the entanglement entropy for the vacuum state of a single scalar field. Second, we consider some maximally entangled states for the two-scalar field system and compute the logarithmic negativity and the mutual information. Qualitative differences of these results pertaining to the charge content of the states are emphasised. Based upon these results, we suggest some possible effects of a background magnetic field on the degradation of entanglement between states in an accelerated frame, for charged quantum fields.
7.	Chaplin, the Dreyfusard AF Dcruz, A Louis - Journal of Popular Film and Television, 2020 **Abstract:** Chaplin's Limelight and A King in New York uncover how political trials often deploy a guilt-by-association strategy. In denouncing such politically motivated charades of justice, Chaplin becomes a Dreyfusard, a term that reminds one of Emile Zola for the anti-establishment stance he maintained during the Dreyfus Affair.
8.	Characterization of MWCNTs-polystyrene nanocomposite based strain sensor T Singla, A Pal Singh, S Kumar, G Singh, N Kumar - Proceedings of the Institution of Mechanical Engineers, Part E, 2020 **Abstract:** The usage of nano phase materials for strain sensing applications has attracted attention due to their unique electromechanical properties. The nanocomposite as piezo-resistive films provides an alternative for the realization of strain sensors with high sensitivity than the conventional sensors based on metal and semiconductor strain gauges. In this work, polymer based nano-composite with carbon nanotubes as filler were developed. The multi-walled carbon nanotubes/polystyrene (MWCNTs/PS) nano-composite films were prepared with different wt.% of CNTs using solution mixing method. Field emission scanning electron microscopy technique was carried out to investigate the morphology and dispersion of CNTs in the nano-composite sample. Fourier transform infrared spectroscopy technique was employed to characterize the bonds present in the prepared nano-composite. The electrical response of the composite films was recorded in the form of current-voltage (I-V) characteristics using source meter. The electromechanical response of the nano-composite films with different wt.% of filler CNTs was

	recorded by applying uni-axial tensile load. The electromechanical responses were then analyzed to obtain gauge factor for the strain sensitivity. The highest gauge factor of 133 was recorded during tensile testing of the nano-composite with 3 wt.% of CNTs fillers.
9.	Deciphering the Structural Enigma of HLA Class-II Binding Peptides for Enhanced Immunoinformatics-based Prediction of Vaccine Epitopes D Chatterjee, P Priyadarshini, DK Das, K Mushtaq, B Singh, JN Agrewala - Journal of Proteome Research, 2020 **Abstract:** Vaccines remain the most efficacious means to avoid and eliminate morbid diseases associated with high morbidity and mortality. Clinical trials indicate the gaining impetus of peptide vaccines against diseases for which an effective treatment still remains obscure. CD4 T-cell-based peptide vaccines involve immunization with antigenic determinants from pathogens or neoplastic cells that possess the ability to elicit a robust T helper cell response, which subsequently activates other arms of the immune system. The available in silico predictors of human leukocyte antigen II (HLA-II) binding peptides are sequence-based techniques, which ostensibly have balanced sensitivity and specificity. Structural analysis and understanding of the cognate peptide and HLA-II interactions are essential to empirically derive a successful peptide vaccine. However, the availability of structure-based epitope prediction algorithms is inadequate compared with sequence-based prediction methods. The present study is an attempt to understand the structural aspects of HLA-II binders by analyzing the Protein Data Bank (PDB) complexes of pHLA-II. Furthermore, we mimic the peptide exchange mechanism and demonstrate the structural implication of an acidic environment on HLA-II binders. Finally, we discuss a structure-guided approach to decipher potential HLA-II binders within an antigenic protein. This strategy may accurately predict the peptide epitopes and thus aid in designing successful peptide vaccines. 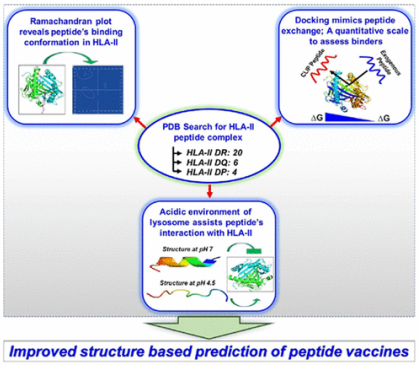
10.	Deep learning networks for capacity estimation for monitoring SOH of Li-ion batteries for electric vehicles K Kaur, A Garg, X Cui, S Singh, BK Panigrahi - International Journal of Energy Research, 2020 **Abstract:** Data-driven modeling using measurable battery signals tends to provide robust battery capacity estimation without delving deep into electrochemical phenomenon inside the battery. Nowadays, with the advent of artificial intelligence, deep neural networks are playing crucial role in data modeling and analysis. In this article, models of three different families of network architectures such as feed-forward neural network (FNN), convolutional neural network (CNN), and long short-term memory neural network (LSTM) are proposed for battery capacity estimation. Measurements from a set of two rechargeable Li-ion batteries are considered for the model performance evaluation. The battery capacity estimation by different models has been

	evaluated by considering the effect of certain parameters such as model complexity, sampling rate of battery measurable signals and type of battery measurable signals. With its ability to process time-series data efficiently by memorizing long-term dependencies, LSTM outperforms other model architectures in estimating battery capacity more accurately and flexibly with 4.69% and 19.16% decline in average test root mean square error (RMSE) as compared with FNN and CNN, respectively. Simpler architectures of LSTM and FNN are able to perform well as compared with CNN, which needs architecture with certain hidden layers to interpret the battery aging process. Moreover, investigations reveal that sparsely sampled battery signals help all the proposed models to learn the battery dynamics in a better way as compared to densely sampled battery signals which also entails for less complex model learning process. Further, among all battery measurable signals, battery temperature has relatively less weightage in estimating battery capacity.
11.	Depth Estimation From Single Image And Semantic Prior P Hambarde, A Dudhane, PW Patil, S Murala, A Dhall - 2020 IEEE International Conference on Image Processing (ICIP), 2020 **Abstract:** The multi-modality sensor fusion technique is an active research area in scene understating. In this work, we explore the RGB image and semantic-map fusion methods for depth estimation. The LiDARs, Kinect, and TOF depth sensors are unable to predict the depth-map at illuminate and monotonous pattern surface. In this paper, we propose a semantic-to-depth generative adversarial network (S2D-GAN) for depth estimation from RGB image and its semantic-map. In the first stage, the proposed S2D-GAN estimates the coarse level depthmap using a semantic-to-coarse-depth generative adversarial network (S2CD-GAN) while the second stage estimates the fine-level depth-map using a cascaded multi-scale spatial pooling network. The experimental analysis of the proposed S2D-GAN performed on NYU-Depth-V2 dataset shows that the proposed S2D-GAN gives outstanding result over existing single image depth estimation and RGB with sparse samples methods. The proposed S2D-GAN also gives efficient results on the real-world indoor and outdoor image depth estimation.
12.	Design, development and evaluation of Artificial Breathing Capability Device (ABCD): a novel innovation for respiratory support JL Mathew, M Sharma, A Gawri, N Kumar, A Chander… - BMJ Innovations, 2020 **Abstract:** Objective: The paucity of mechanical ventilators necessitates development of innovative respiratory support devices. Methods: We developed the Artificial Breathing Capability Device (ABCD) to automate compression of self-inflating bags (SIB), while controlling peak inspiratory pressure (PIP), ventilation rate (VR) and inspiration to expiration time (I:E) ratio (as in a conventional ventilator). ABCD has additional smart features including self-regulatory checks, auto cut-off during cough, endotracheal tube disconnection and blockage alarms, and SIB disconnection alarm. ABCD was tested non-stop for 60 days with 396 user combinations, using adult-size and paediatric-size SIB. The device was evaluated for robustness, reliability and precision. Results: ABCD did not have mechanical, electrical or electronic failures during continuous testing under various ambient conditions, confirming robustness. Reliability and precision evaluated by the proportion of user combinations showing <10% deviation from the set parameters showed: PIP 100%, VR 100% and I:E 84.3% with an adult SIB. The corresponding proportions with a paediatric-size SIB were 85.4%, 100% and 95.5%. With both SIB, the only combinations showing >10% deviation were outside the physiologic range.

	Conclusion: ABCD is a safe, efficacious and cost-effective option, which could be considered for adults and children in the context of ventilator shortages especially during the COVID-19 pandemic.
13.	Design of NFRP Based SIR-Loaded Two Element MIMO Antenna System for 28/38 GHz sub mm-wave 5G Applications R Chandra, D Sarkar, D Ganguly, C Saha, JY Siddiqui… - IEEE 3rd 5G World Forum (5GWF), 2020 **Abstract:** Design of a compact dual band (28/38 GHz) antenna for sub mm-wave 5G application employing near field resonant parasitic (NFRP) excitation is reported in this article. Two differently sized electrically small stepped impedance resonators (SIR), loaded beneath the substrate and above the superstrate respectively, and parasitically excited by a monopole printed on the top side of the substrate, constitute the basic antenna element contributing to the dual band performance at 28 and 38 GHz. This basic antenna element is further deployed to realize a 2-element MIMO antenna exhibiting excellent impedance and radiation characteristics over both the bands. The design is currently under further investigation and experimental results would be presented during the conference. The proposed antenna exhibiting impedance bandwidth of 3.5 GHz and 1.5 GHz centred at 28 GHz and 38 GHz respectively with satisfactorily low mutual coupling and ECC can serve as a subarray for 5G massive MIMO base stations.
14.	Disentangling complete and incomplete fusion events in $^{12} $ C+ $^{169} $ Tm reaction by spin-distribution measurements A Sood, S Thakur, A Sharma, VR Sharma, A Yadav…PP Singh… - Journal of Physics G: Nuclear and Particle Physics, 2020 **Abstract:** The spin-distributions of different reaction products populated via xn and α/2$\alpha$$x$n channels in ^{12}C+^{169}Tm system have been measured at E$_{lab} \approx$ 6, 7 and 7.5 MeV/A. Particle(p,α)-γ-coincidences were recorded to identify evaporation residues channel-by-channel. The spin-distributions of fusion evaporation and direct-α-emitting channels are found to be distinct corroborating the involvement of entirely different reaction dynamics in their production, respectively termed as complete (CF) and incomplete fusion (ICF). The values of mean input angular momenta, obtained from the analysis of the spin-distributions, involved in ICF- α/2αxn channels are estimated to be larger than that observed in CF-xn/αxn channels. For ICF-α/2αxn channels, the multiplicity of fast-α particle emission increases with the magnitude of input angular momentum imparted into the system. The CF residues display a population of broad spin range while the ICF residues are confined to a narrow spin range generally localized in the higher spin states. Findings of the present work conclusively demonstrate the possibility to populate high spin states in final reaction products using ICF, which are otherwise not accessible. Further, an attempt has been made to study the variation of input angular momentum with the choice of different entrance-channel parameters. It has been observed that the value of input angular momentum involved in ICF- α/2αxn channels increases with the deformation and entrance-channel mass-asymmetry parameter, indicating strong entrance-channel dependence of ICF dynamics.

15.	Efficient Dispersion on an Anonymous Ring in the Presence of Weak Byzantine Robots AR Molla, K Mondal, WK Moses - International Symposium on Algorithms and Experiments for Sensor Systems, Wireless Networks and Distributed Robotics: Algorithms for Sensor Systems, Part of the Lecture Notes in Computer Science book series, 2020 **Abstract:** The problem of dispersion of mobile robots on a graph asks that n robots initially placed arbitrarily on the nodes of an n-node anonymous graph, autonomously move to reach a final configuration where exactly each node has at most one robot on it. This problem has been relatively well-studied when robots are non-faulty. In this paper, we introduce the notion of Byzantine faults to this problem, i.e., we formalize the problem of dispersion in the presence of up to f Byzantine robots. We then study the problem on a ring while simultaneously optimizing the time complexity of algorithms and the memory requirement per robot. Specifically, we design deterministic algorithms that attempt to match the time lower bound ($\Omega(n)$ rounds) and memory lower bound ($\Omega(\log n)$ bits per robot). Our main result is a deterministic algorithm that is both time and memory optimal, i.e., $O(n)$ rounds and $O(\log n)$ bits of memory required per robot, subject to certain constraints. We subsequently provide results that require less assumptions but are either only time or memory optimal but not both. We also provide a primitive that takes robots initially gathered at a node of the ring and disperses them in a time and memory optimal manner without additional assumptions required .
16.	Eigenfunctions and genetic algorithm based improved strategies for performance analysis and geometric optimization of a two-zone solar pond A Kumar, S Verma, R Das - Solar Energy, 2020 **Abstract:** In this paper, concept of a modified two-zone solar pond consisting lateral extraction from an extended length of convection free zone combined with thermoelectric generators for electrical power generation is proposed. In this work, a new transient-state analytical model to predict the performance of such a system is developed. Fully closed-form transient solution for performance analysis during extended length lateral heat extraction from solar ponds is not yet available in the literature. The presence of two source terms, one of which is solution dependent and mixed boundary conditions makes the present study complex to be solved analytically. The methodology based on the expansion of Eigenfunctions is proposed to predict temperature profiles within the solar pond having dual layer heat extraction. Using the temperature field, net energy output from the system for a specified period is obtained. The variation in power output and net energy for various cases of design and operating parameters during the maturation phase of the solar pond and after achieving the steady-state is analysed. The sensitivity of different operating and design parameters on the output of the system is also evaluated. Further, an inverse optimization analysis is also carried out to search for possible combinations of various design and operating parameters in the system towards meeting a specified net energy output from the thermoelectric generators. It was observed that using the inversely obtained set of parameters can significantly reduce the volume, base area, and total height of the solar pond concerning the existing convention.
17.	Estimating Per-Unit-Length Resistance Parameter in Emerging Copper-Graphene Hybrid Interconnects via Prior Knowledge based Accelerated Neural Networks R Kumar, SSL Narayan, S Kumar, S Roy, BK Kaushik…R Sharma - IEEE 29th Conference on Electrical Performance of Electronic Packaging and Systems (EPEPS), 2020

	Abstract: In this paper, an artificial neural network (ANN) is developed to model how the geometrical parameters of hybrid copper-graphene interconnects affect the per-unit-length resistance values. The proposed ANN is intelligently trained using large amounts of data representing the prior knowledge about the interconnects, extracted from an analytical model and sparse amount of data extracted from a rigorous full-wave electromagnetic solver. In this way, the training of the ANN model is accelerated without significant loss in accuracy.
18.	Event Detection and Localization for Sparsely Populated Outdoor Environment Using Seismic Sensor P Choudhary, N Goel, M Saini - IEEE Sixth International Conference on Multimedia Big Data (BigMM), 2020 **Abstract:** Accurate event detection and localization is one of the key requirements for multiple smart applications. In this paper, we present a framework for event detection and localization using seismic sensors in an outdoor environment. Seismic sensors have been widely used for event detection. This paper extends the application of seismic sensor for localization. We develop a framework using multiple seismic sensors and fuse the information to detect and localize a target. The proposed framework employs regression and property of seismic waves for localization. We develop a prototype system to verify the proposed methods. The event detection module shows the average detection accuracy of 96% whereas localization modules show average localization error 1.37 meters.
19.	FORTRESS: FORTRAN programs for solving coupled Gross-Pitaevskii equations for spin-orbit coupled spin-1 Bose-Einstein condensate P Kaur, A Roy, S Gautam - Computer Physics Communications, 2021 **Abstract:** Here, we present simple and efficient numerical scheme to study static and dynamic properties of spin-1 Bose–Einstein condensates (BECs) with spin–orbit (SO) coupling by solving three coupled Gross–Pitaevskii equations (CGPEs) in three-, quasi-two and quasi-one dimensional systems. We provide a set of three codes developed in FORTRAN 90/95 programming language with user defined ‘option’ of imaginary and real-time propagation. We present the numerical results for energy, chemical potentials, and component densities for the ground state and compare with the available results from the literature. The results are presented for both the ferromagnetic and antiferromagnetic spin-1 BECs with and without SO coupling. To improve the computational speed, all the codes have the option of OpenMP parallelization. We have also presented the results for speedup and efficiency of OpenMP parallelization for the three codes with both imaginary and real-time propagation.
20.	Forward and Inverse Analyses of Two-Dimensional Eccentric Annular Fins for Space-Restriction Circumstances R Das, B Kundu - Journal of Thermophysics and Heat Transfer, 2020 **Abstract:** Heat transfer under space restriction is a challenging task in many energy systems due to unavoidable design constraints. For such conditions, the use of regular fin shapes cannot be possible, and eccentric geometry becomes a necessity. In this work, an optimization technique based on the inverse analysis using the differential evolution (DE) has been proposed to identify the dimensions of two-dimensional eccentric annular disk fins. For maximizing the rate of energy transport under a prescribed volume, DE search is first used in the present paper to discover numerous combinations of critical geometrical variables satisfying a constrained volume. Thereafter, all parameters relating to the energy transport are obtained from a direct analysis aided by a semi-analytical technique. It is envisaged from the current inverse analysis

	that under a given volume of the fin, although the same maximum value of heat transmission rate can be acquired with multiple combinations of fin dimensions, there is a sufficient scope to minimize the fin surface area. Here, the optimized temperature contour acts as a significant cause in selecting the unique combination of the optimized fin geometry. Finally, the role of fin thickness is found more influential to control the rate of energy exchange.
21.	Gender Differences in Work Trip Generation: Evidences from Bangalore TM Rahul, TM Megha, S Meenakshi… - Transportation Research Procedia, 2020 **Abstract:** Many of the existing travel behavior models fall short in characterizing the gender differences in transportation. Understanding these differences aids development of sustainable cities typically from a social equity perspective. In this research paper, authors identify a modeling framework to determine the work choice propensity among females in the city of Bangalore. An initial data analysis provides a descriptive variation of the work choice propensity among males and females, and the further regression models elicits the impact of various factors on the work choice propensity of individuals. In the regression framework, the interaction model examines the existence of gendered variation in the influence of various factors, and subsequent models estimates the influence of these factors separately for males and females. The significant impact of the gender incorporated interaction terms in the study reflected the need for gender specific market segment. Further, the stronger influence of social conformation factors on the work choice of women indicated the need for flexible working hours and childcare facilities at work for women. In a developing country context, the study also elicited the role of awareness and educational programs to revamp the societal attitudes, rooted on the patriarchal mind-set, against women's work participation.
22.	Graphene as a nanoelectromechanical reference piezoresistor A Sinha, A Sharma, P Priyadarshi, A Tulapurkar… - Physical Review Research, 2020 **Abstract:** Motivated by the recent prediction of anisotropy in piezoresistance of ballistic graphene along longitudinal and transverse directions, we investigate the angular gauge factor of graphene in the ballistic and diffusive regimes using highly efficient quantum transport models. It is shown that the angular gauge factor in both ballistic and diffusive graphene between 0° to 90° bears a sinusoidal relation with a periodicity of π due to the reduction of sixfold symmetry into a twofold symmetry as a result of applied strain. The angular gauge factor is zero at critical angles 20° and 56° in ballistic and diffusive regimes, respectively. Based on these findings, we propose a graphene-based ballistic nanosensor which can be used as a reference piezoresistor in a Wheatstone bridge readout technique. The reference sensors proposed here are unsusceptible to inherent residual strain present in strain sensors and unwanted strain generated by the vapors in explosives detection. The theoretical models developed in this paper can be applied to explore similar applications in other two-dimensional Dirac materials. The proposals made here potentially pave the way for implementation of nanoelectromechanical strain sensors based on the principle of ballistic transport, which will eventually replace conventional microelectromechanical piezoresistance sensors with a decrease in feature size. The presence of strain-insensitive "critical angle" in graphene may be useful in flexible wearable electronics also.
23.	Highly efficient visible-light-driven reduction of Cr (vi) from water by porphyrin-based metal–organic frameworks: effect of band gap engineering on the photocatalytic activity N Sharma, AK Dey, RY Sathe, A Kumar, V Krishnan, TJD Kumar, CM Nagaraja - Catalysis Science & Technology, 2020 **Abstract:** Highly efficient visible-light-assisted photocatalytic reduction of Cr(VI) to Cr(III)

	from water using multifunctional Zr(IV)-porphyrin MOFs, Zr6(μ3-OH)8(OH)8(MTCPP)2, (PCN-222(M)) (M = H2, ZnII, CuII, NiII, CoII, FeIIICl, and MnIIICl) is presented. The remarkable chemical stability of these Zr-MOFs in water and the visible-light harvesting property of the porphyrin-linker promoted efficient photocatalytic activity for the reduction of Cr(VI) to Cr(III) in the aqueous phase. Interestingly, the pristine MOF, PCN-222, showed an unprecedentedly high photocatalytic activity with 100% reduction of Cr(VI) to Cr(III) within 25 min with the highest rate (0.1289 min−1) amongst the MOFs reported so far. The superior photocatalytic activity of PCN-222 (no metal) over PCN-222(M) MOFs has been attributed to its lower band gap and efficient transfer of photo-excited electrons to the catalytic site, supported by combined experimental and theoretical studies. Remarkably, the PCN-222 MOF catalyst could be reused for up to 10 cycles without significant loss of catalytic activity. Further, a detailed mechanistic investigation of the visible light-assisted photoreduction of Cr(VI) by combined experimental and theoretical studies is presented. Overall, this work represents a unique demonstration of the influence of band gap engineering of porphyrin MOFs for efficient aqueous-phase photoreduction of Cr(VI) from water under visible light irradiation.
24.	Highly elastic, electroconductive, immunomodulatory graphene crosslinked collagen cryogel for spinal cord regeneration G Agarwal, N Kumar, A Srivastava - Materials Science and Engineering: C, 2020 **Abstract:** Novel amino-functionalized graphene crosslinked collagen based nerve conduit having appropriate electric (3.8 ± 0.2 mSiemens/cm) and mechanical cues (having young modulus value of 100–347 kPa) for stem cell transplantation and neural tissue regeneration was fabricated using cryogelation. The developed conduit has shown sufficiently high porosity with interconnectivity between the pores. Raman spectroscopy analysis revealed the increase in orderliness and crosslinking of collagen molecules in the developed cryogel due to the incorporation of amino-functionalized graphene. BM-MSCs grown on graphene collagen cryogels have shown enhanced expression of CD90 and CD73 gene upon electric stimulation (100 mV/mm) contributing towards maintaining their stemness. Furthermore, an increased secretion of ATP from BM-MSCs grown on graphene collagen cryogel was also observed upon electric stimulation that may help in regeneration of neurons and immuno-modulation. Neuronal differentiation of BM-MSCs on graphene collagen cryogel in the presence of electric stimulus showed an enhanced expression of MAP-2 kinase and β-tubulin III. Immunohistochemistry studies have also demonstrated the improved neuronal differentiation of BM-MSCs. BM-MSCs grown on electro-conductive collagen cryogels under inflammatory microenvironment in vitro showed high indoleamine 2,3 dioxygenase activity. Moreover, macrophages cells grown on graphene collagen cryogels have shown high CD206 (M2 polarization marker) and CD163 (M2 polarization marker) and low CD86 (M1 polarization marker) gene expression demonstrating M2 polarization of macrophages, which may aid in tissue repair. In an organotypic culture, the developed cryogel conduit has supported cellular growth and migration from adult rat spinal cord. Thus, this novel electro-conductive graphene collagen cryogels have potential for suppressing the neuro-inflammation and promoting the neuronal cellular migration and proliferation, which is a major barrier during the spinal cord regeneration. **Graphical Abstract:** Graphene crosslinked collagen based nerve conduit promotes collagen orderliness, alternatively activated macrophages differentiation, BM-MSCs differentiation and release ATP and support spinal cord regeneration.

	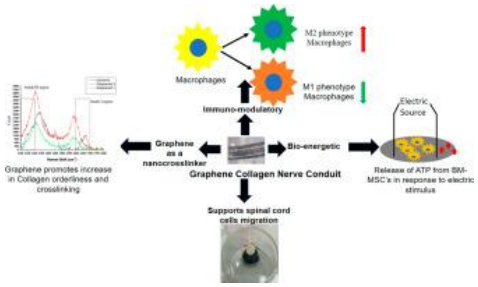
25.	Independent component analysis for pulse compressed frequency modulated thermal wave imaging for inspection of mild steel K Kaur, R Mulaveesala, A Rani, V Kher - IOP SciNotes, 2020 **Abstract:** Non-destructive testing & evaluation plays a crucial role in various sectors for testing the reliability of materials. Of the different available non-destructive examination techniques, thermal non-destructive testing provides fast and remote inspection of the materials. Among various widely used thermal non-destructive testing techniques, frequency modulated thermal wave imaging gained its importance due to its higher test sensitivity and resolution. The adopted matched filter approach on the obtained temporal temperature distribution further concentrates supplied excitation energy into a narrow duration high peak power pulse. In this paper, the merits of the reconstructed high peak power pulsed data have been considered and emphasized in the context of independent component analysis. The obtained results clearly indicate that pulse compressed data improves defect detectability, reliability, memory usage, and computational complexity
26.	Investigation of fusion probabilities in the reactions with Cr 52, 54, Ni 64, and Zn 68 ions leading to the formation of Z= 120 superheavy composite systems KV Novikov, EM Kozulin, GN Knyazheva, IM Itkis…PP Singh, RN Sahoo… - Physical Review C, 2020 **Abstract:** Background: The formation of superheavy nuclei in fusion reactions is suppressed by a competing quasifission process. The competition between the formation of the compound nucleus and the quasifission depends strongly on the reaction entrance channel. Purpose: The investigation of fission and quasifission processes in the formation of Z=120 superheavy composite systems in the 52,54Cr+248Cm and 68Zn+232Th reactions, and their comparison with the 64Ni+238U reaction at energies in the vicinity of the Coulomb barrier. Methods: Mass-energy distributions of fissionlike fragments formed in the reactions 52,54Cr+248Cm and 68Zn+232Th at energies near the Coulomb barrier were measured using the double-arm time-of-flight spectrometer CORSET. Results: Capture cross sections for the reactions under investigation were measured. The most probable fragment masses and total kinetic energies as well as their variances in dependence on the interaction energy were studied for asymmetric and symmetric fragments. The fusion probabilities were estimated from the analysis of mass-energy distributions. Conclusions: The estimated fusion probability drops down by a factor of 103 in the 54Cr+248Cm reaction compared to the reactions of 48Ca ions with actinides. Among the studied reactions, the 54Cr+248Cm is the most favorable one for the production of the superheavy element with Z=120.

27.	Investigation of Nature of Cyclic Combustion Variations in RCCI Engine A Singh, MR Saxena, RK Maurya - National Conference on IC Engines and Combustion: Advances in IC Engines and Combustion Technology, Part of the Lecture Notes in Mechanical Engineering book series, 2020 **Abstract:** This paper presents the investigation of the nature of cyclic combustion variations in gasoline–diesel RCCI engine. An automotive diesel engine is modified with suitable hardware modifications and instrumentation to operate it in reactivity controlled compression ignition (RCCI) combustion mode. A development electronic control unit (ECU) is used to control the fuel injection events. The experiments were performed at a constant engine speed of 1500 rpm and engine load of 1.5 bar BMEP for various diesel injection timings with single and double injection strategy. In-cylinder pressure history of 1000 consecutive engine cycles is recorded for combustion stability analysis. The return map technique is used for determining the nature of combustion stability in total heat release (THR) of gasoline–diesel RCCI engine. The results depict the presence of randomness for retarded injection timings and correlations for advanced injection timings where cyclic variations are too high.
28.	Large Scale Hierarchical Anomaly Detection and Temporal Localization S Kanwal, V Mehta, A Dhall - Proceedings of the 28th ACM International Conference on Multimedia, 2020 **Abstract:** Abnormal event detection is a non-trivial task in machine learning. The primary reason behind this is that the abnormal class occurs sparsely, and its temporal location may not be available. In this paper, we propose a multiple feature-based approach for CitySCENE challenge-based anomaly detection. For motion and context information, Res3D and Res101 architectures are used. Object-level information is extracted by object detection feature-based pooling. Fusion of three channels above gives relatively high performance on the challenge Test set for the general anomaly task. We also show how our method can be used for temporal localisation of the abnormal activity event in a video.
29.	Modification of tensor force in 0p-shell model effective interaction K Jha, P Kumar, S Sarkar, PK Raina - International Journal of Modern Physics E, 2020 **Abstract:** In many shell model interactions, the tensor force monopole matrix elements often retain systematic trends originating in the bare tensor force. However, in this work, we find that Isospin T=0 tensor force monopole matrix elements of widely used p-shell effective interaction CK(8–16) do not share these systematic. We correct these discrepancies by modifying T=0 tensor force two-body matrix elements (TBMEs) of CK(8–16) by the analytically calculated tensor force TBMEs. With some additional modification of single-particle energies and TBMEs, the revised effective interaction is named as CKN. The effective interaction CKN has been tested for the calculations of p-shell nuclei of normal parity states from various physics viewpoints such as excitation spectra, electromagnetic moments, and electromagnetic and Gamow–Teller (GT) transitions. The obtained results are found to be satisfactory with respect to the experimental results.
30.	Multivariate Adaptive Gaussian Mixture for Scene Level Anomaly Modeling P Kumari, M Saini - IEEE Sixth International Conference on Multimedia Big Data (BigMM), 2020 **Abstract:** Scene changes that typically occur in a real-world setting degrade anomaly detection performance over the long run. Most of the existing methods ignore the challenge of temporal

	concept drift in video surveillance. In this paper, we propose an unsupervised end-to-end framework for adaptive scene level anomaly detection. We utilize multivariate Gaussian mixtures for adaptive scene learning. The mixture represents the possible distribution of normal and abnormal events shown till now. The distribution adapts itself according to the slow scene changes. We introduce a Mahalanobis distance-based contribution factor to update mixture parameters on the arrival of each new event. A detailed discussion and experiments are conducted to decide optimum local as well as global temporal context. The existing public datasets for anomaly detection are of very short duration (maximum of 1.5 hours) to be used for evaluating adaptive approaches. Therefore we also collected a longer duration dataset of continuous 10 hours duration. We achieved a promising performance of 85.14% AUC and 21.26% EER on this data.
31.	Nanoscale charge transport and local surface potential distribution to probe the defect passivation in Cr-substituted earth abundant CZTS absorber layer K Kaur, AH Chowdhury, Q Qiao, M Kumar - Journal of Alloys and Compounds, 2020 **Abstract:** The non-stochiometric deviations in CZTS often results in certain detrimental point defects that act as trap centers causing non-radiative recombination and potential fluctuations, eventually results in large open circuit voltage (VOC) deficit in CZTS solar cells. Cationic substitution in CZTS layer is one of the leading approaches to capture the great potential of kesterite solar cells for future cost-effective photovoltaic technology. Here, chromium incorporation in CZTS is studied for cationic substitution in CZTS layer, as it renders multiple chemical states including +1, +2 and + 4 of Cu, Zn and Sn cations in CZTS. The CZTS films determine to have good crystallinity and morphology with no significant disparity among pristine and Cr-doped CZTS films, apart from slight shift of XRD (112) peak indicating partial cation substitution by smaller Cr atoms. However, the Zn content is found to be decreased with increasing Cr content in CZTS layer. Substantial enhancement in the absorption of Cr-doped CZTS films indicate intermediate band (IB) within the band gap. Photoluminescence (PL) emission spectra strongly suggests reduced non-radiative recombination and potential fluctuations in Cr-CZTS films. X-ray photoelectron spectroscopy investigations reveal Zn substitution by Cr in CZTS crystal geometry. Using nanoscale Kelvin Probe Force Microscopy (KPFM) and Conducting Atomic Force Microscopy (CAFM), we verify the surface potential variation and nanoscale electrical conductivity in pristine and Cr-CZTS films. Additionally, Zn substitution by Cr eventually lead to suppression of ZnSn deep level defects segregated at grain boundaries (GBs). CAFM strongly confirms the GB passivation in Cr-CZTS films. This work widens the opportunity of exploring potential cationic substitution in CZTS for developing high efficiency CZTS solar cells.
32.	Nanosensors for gas sensing applications M Kumar, AV Agrawal, M Moradi, R Yousefi - Nanomaterials for Air Remediation, 2020 **Abstract:** Semiconductor-based gas sensors are the important family of electronic devices that are widely used in various sciences and industries. The basic principles of this type of sensor are based on the reaction of the gas molecules and the semiconductor surface. Therefore, nanostructured semiconductors are the best candidate for fabricating of this type of gas sensor due to their high surface area/volume ratio. Of these types of semiconductors, metal-oxides semiconductors (MOS) such as zinc oxide (ZnO) and transition metal dichalcogenides (TMD) such as molybdenum disulfide (MoS2) (or moly) are very important. Therefore, in this chapter the recent findings of these types of sensors will be presented and discussed. The capability of MoS2 nanostructures as a member of TMDs to detect different gases such as H2 and NO2 has

	been presented. We presented that, how hybrid MoS2 shown better gas sensing performance in comparison the pristine MoS2. In the next step, ZnO nanostructures from MOS family have been chosen to study their gas sensing applications to detect ammonia, acetic acid, ethanol, and methanol. In addition, the effects of graphene as a 2-dimensional (2D) structure on gas sensing performance of ZnO nanostructures have been discussed. Furthermore, it has been shown how the gas sensing performance of ZnO nanostructures could be improved by an organic semiconductor such as polyaniline (PAni).
33.	New Forward and Inverse Solutions for Wet Fins of Generalized Profiles with All Nonlinear Phenomena R Das, B Kundu - Journal of Heat Transfer, 2020 **Abstract:** This study establishes forward closed-form and inverse analyses of wet fins of various profiles involving all modes of heat transfer. Existing limitations in the literature address here by choosing the appropriate nonlinear variation of thermal conductivity and radiation effects. The error between linear and nonlinear methodologies is found to be within 60%. Furthermore, the maximum error between the closed-form solution based on the Differential Transformation Method (DTM), and the numerical solution is observed as 0.5%. After necessary validations, optimization of various fin profiles is carried out by the maximization of the net fin heat transmission rate under a defined fin volume and thermo-geometrical constraints. For the optimum criterion, the suitability of the Artificial Bee Colony (ABC)-based meta-heuristic technique is established. To satisfy the volumetric constraint, the objective function of ABC lesser than O(10-5) is found sufficient. The identification of thermo-geometrical parameters is realized by analyzing combinations obtained from 100 runs of ABC and the decision-making criterion is adopted on the basis of the maximum thermal performance. Among the studied profiles, concave parabolic geometry yields the maximum heat transport rate, which is followed by triangular, convex, and rectangular geometries for the same fin volume. The present combination of DTM and ABC techniques proposes to be useful in practical applications towards design and the selection of evaporator fins for air-conditioning and refrigeration appliances operating under wet conditions in a more accurate and optimized manner.
34.	Nuclear matrix elements for the λ mechanism of 0νββ decay of ^{48}Ca in the nuclear shell-model: Closure versus nonclosure approach S Sarkar, Y Iwata, PK Raina - Physical Review C, 2020 **Abstract:** The λ and mββ mechanisms of neutrinoless double beta decay (0νββ) occur with light neutrino exchange via WL−WR and WL−WL mediation, respectively. In the present study, we calculate the nuclear matrix elements (NMEs) for the mββ and λ mechanisms of 0νββ, which has origin in the left-right symmetric model with right-handed gauge boson at TeV scale. The NMEs are calculated for one of the 0νββ decaying isotope 48Ca in the interacting nuclear shell-model using the GXPF1A effective interaction of pf shell. The NMEs are calculated in both closure and nonclosure approaches using four different methods: closure, running closure, running nonclosure, and mixed methods. All the NMEs are calculated incorporating the effects of the finite size of nucleons and the revisited higher-order terms such as pseudoscalar and weak magnetism terms of the nucleon currents. Inclusion of the short-range nature of nucleon-nucleon interaction in Miller-Spencer, CD-Bonn, and AV18 parametrizations is also taken care of. We have used closure energy ⟨E⟩=0.5 MeV, which is near to the optimal value of closure energy that is extracted by examining the dependence of NMEs with closure energy in closure and mixed methods. The comparative dependence of the running closure and running nonclosure NMEs with the spin-parity of the allowed states of intermediate nucleus 48Sc, the coupled spin-parity of

	the two initial decaying neutrons and the final two protons, the cutoff excitation energy of 48Sc, and the cutoff number of states of 48Sc are examined. The neutrino momentum and radial distribution of different types of NMEs are explored. It is found that there is a significant enhancement in MqGT-type NMEs, which originates from the large momentum distribution for the inclusion of the higher-order pseudoscalar term of the nucleon currents.
35.	On the Dependence of Critical Velocity on the Material Properties During Cold Spray Process L Palodhi, H Singh - Journal of Thermal Spray Technology, 2020 **Abstract:** Optimization of the cold spray process is extremely challenging due to the involvement of a large number of process parameters as well as material properties. Modern approaches for modeling the cold spray process have relied largely on numerical simulations. In this paper, we shall present a simplified mathematical model which will be benchmarked against experimental and numerical measurements available in the literature and demonstrate that the model shows reasonable agreement with real-world observations. We will present a parametric study using this model and identify the factors that strongly affect the cold spray process, which can be used for identifying and optimizing the process parameters and the material properties.
36.	Physical Model Based Method to Generate Channel Coefficients for Nakagami-m Distribution B Kumbhani, J Gaur - Wireless Personal Communications, 2020 **Abstract:** In this paper, we discuss physical model based method to generate channel coefficients for Nakagami-m distribution. We consider the phase envelope joint distribution so that the phase of the faded signal is also considered. Mainly, the coefficients are generated by exploring the physical model that relates the Nakagami-m fading distribution with Gaussian and gamma distributions for which generation of coefficients is available in commonly used simulation tools. The empirical probability density function (PDF) of generated coefficients are compared with the theoretical values and they are found in excellent agreements. The empirical PDFs for envelope and phase of the generated coefficients are validated using the Kolmogorov–Smirnov test.
37.	Probability of Detecting the Deep Defects in Steel Sample using Frequency Modulated Independent Component Thermography J Ahmad, A Akula, R Mulaveesala, HK Sardana - IEEE Sensors Journal, 2020 **Abstract:** Active thermography is a widely used non-destructive testing and evaluation technique (NDT&E) for evaluating the properties of materials without impairing its future usefulness. In this work, a mild steel sample made of artificial flat-bottom holes at varied depths, was examined with the emerging non-stationary thermal wave imaging (NSTWI) technique, i.e. frequency modulated thermal wave imaging (FMTWI).The pulse compression favorable of NSTWI technique is eminent for compressing the applied thermal energy into a narrow-compressed pulseto enhance the depth resolution and sensitivity. In this work, pulse compressed thermographic data generated from FMTWI experimentation is analyzed with the unsupervised learning approach independent component analysis (ICA) to test their mutual return in the detection of the deep defects in a mild steel sample and this proposed technique was referred to as frequency modulated independent component thermography (FMICT). In comparison, the effect of FMICT was contrasted with othermethodsi.e. pulse compression of time domain and ICA of feature space by considering the signal-to-noise ratio (SNR) as a figure of merit. Furthermore, a probability of detection (POD) analysis framework based on the minimum threshold SNR criteria for apparent visibility of the defects has been presented to assess the probability of identifying defects at various depths using such approaches. The influence of the

	SNR threshold value for the above strategies on the POD curves has also been presented.
38.	QWiki: A Collaborative Space to Mine Feedback for MOOCs S Setia, SRS Iyengar, A Agarwal - Proceedings of the 21st Annual Conference on Information Technology Education, 2020 **Abstract:** In a classroom environment, "understood?" is the most common feedback question asked by a teacher for the evaluation of his/her teaching. But, in a virtual environment like MOOCs, no such feedback mechanism can be materialized. In this paper, we propose that a combination of wiki and QnA forum (called QWiki) can be used to mine feedback for the video lectures. The results of the experiment show that the deployment of a collaborative space like QWiki in MOOCs helps to judge the degree of comprehension of the concepts in the video lectures by the students.
39.	Ramanujan–Petersson conjecture for Fourier–Jacobi coefficients of Siegel cusp forms B Kumar, B Paul - Bulletin of the London Mathematical Society **Abstract:** Let FF be a Siegel cusp form of weight kk and degree n>1n>1 with Fourier-Jacobi coefficients $\{\phi m\}m\in\mathbb{N}\{\phi m\}m\in N$. In this article, we investigate the Ramanujan–Petersson conjecture (formulated by Kohnen) for the Petersson norm of $\phi m\phi m$. In particular, we show that this conjecture is true when FF is a Hecke eigenform and a Duke–Imamoğlu–Ikeda lift. This generalizes a result of Kohnen and Sengupta. Further, we investigate an omega result and a lower bound for the Petersson norms of $\phi m\phi m$ as $m\to\infty m\to\infty$. Interestingly, these results are different depending on whether FF is a Saito–Kurokawa lift or a Duke–Imamoğlu–Ikeda lift of degree $n\geqslant 4n\geqslant 4$.
40.	Readiness self-assessment of cement industry for sustainable manufacturing implementation: A case study of India V Bhakar, KS Sangwan, AK Digalwar - Procedia CIRP, 2020 **Abstract:** An important first step when embarking on the sustainability improvement journey is readiness assessment. Performing readiness assessment is a systematic analysis of an organizations' abilities to undertake the potential sustainability improvement initiatives by identifying the weak areas of the organization and helps to mitigate or close these weak areas before the implementation. However, the cement manufacturing industry is a key player in Indian industry and involves many environmental, social and economic impacts. The cement manufacturing process is also a high energy and resource consuming process. The current study assessed the readiness of Indian cement industry for the overall sustainability improvement. The model provided by Sangwan et al. (2018) for sustainability readiness self-assessment has been adapted for the assessment. An offline survey among a cross functional team of experts from a large cement company was carried out for collecting data on the readiness assessment questions along with real time observations at different plant locations of the company. It is observed that the case organization is doing well and is ready for adopting sustainability improvement initiatives but it needs to focus on developing water related policies for better sustainability. The results provide a complete visualization for the sustainability improvement initiatives in terms of seven resources of air, water, infrastructure, energy, material, money, and people. This readiness assessment tool was found to be simple to use by the managerial/supervisory level employees for the self-assessment of organizational preparedness.

41.	Role of neutron transfer in sub-barrier fusion RN Sahoo, M Kaushik, A Sood…RG Pillay…PP Singh – Physical Review C, 2020 **Abstract:** The fusion excitation function of ^{35}Cl + ^{130}Te system has been measured in a wide energy range, i.e., Ec.m. = 94–121.6 MeV, from sub-barrier to above-barrier energies and compared with the ^{37}Cl + ^{130}Te system to investigate the role of neutron transfer channels in sub-barrier fusion cross-section enhancement. In comparison, the reduced fusion excitation function of ^{35}Cl + ^{130}Te system shows a significant enhancement over the ^{37}Cl + ^{130}Te system at sub-barrier energies. This enhancement is correlated with the presence of six positive Q-value neutron transfer channels in the ^{35}Cl + ^{130}Te system compared to none in the ^{37}Cl + ^{130}Te system. Aiming to probe how fusion at sub-barrier energies responds to different coupling schemes, the excitation functions of both the systems have been analyzed in the framework of the coupled-channels approach on the same footing. The results and coupled-channels analysis presented in this work hints towards the importance of neutron transfer channels in sub-barrier fusion in addition to the inclusion of inelastic excitations of interacting partners. The findings of this work are discussed in light of the conclusions presented by Kohley et al. [Phys. Rev. Lett. 107, 202701 (2011)], in which the role of positive Q-value neutron transfer channels in sub-barrier fusion was studied.
42.	Role of neutron transfer in the sub-barrier fusion cross section in ^{18}O + ^{116}Sn NK Deb, K Kalita, H Al Rashid, S Nath, J Gehlot…RN Sahoo… - Physical Review C, 2020 **Abstract:** Background: In heavy-ion-induced fusion reactions, cross sections in the sub-barrier region are enhanced compared to predictions of the one-dimensional barrier penetration model. This enhancement is often understood by invoking deformation and coupling of the relative motion with low-lying inelastic states of the reaction partners. However, effects of nucleon transfer on fusion below the barrier, especially for the systems having positive Q value neutron transfer (PQNT) channels, are yet to be disentangled completely. Purpose: We intend to study the role of the PQNT effect on the sub-barrier fusion of the 18O + 116Sn system having positive Q value for the two-neutron stripping channel. Also we reflect on the interplay of couplings involved in the system around the Coulomb barrier. Method: The fusion excitation function was measured at energies from 11% below to 46% above the Coulomb barrier for 18O + 116Sn using a recoil mass spectrometer, viz., the Heavy-Ion Reaction Analyser (HIRA). Fusion barrier distributions were extracted from the data. Results from the experiment were analyzed within the framework of the coupled-channels model. Results: Fusion cross sections at energies below the Coulomb barrier showed strong enhancement compared to predictions of the one-dimensional barrier penetration model. The fusion process is influenced by couplings to the collective excitations with coupling to single- and two-phonon vibrational states of the target and the projectile respectively. Inclusion of the two-neutron transfer channel in the calculation along with these couplings could reproduce the data satisfactorily. Conclusions: The significant role of PQNT in enhancing the sub-barrier fusion cross section for the chosen system is not observed. It simply reduced the sub-barrier fusion cross section. Therefore, a consistent link between PQNT and sub-barrier fusion enhancement could not be established vividly while comparing the fusion excitation function from this work with the same from other 16,18O-induced reactions. This clearly points to the need for more experimental as well as theoretical investigation in this field.

43.	Selective-frequency-gap-induced negative anisotropic scattering in designer photonic structures with short-range order SK Saini, RV Nair - Physical Review A, 2020 **Abstract:** Optimizing scattering is the most sought-after goal in wave transport through photonic structures, which opens up many physical processes with prospective applications. Here, we uncover the appearance of a tunable frequency gap with negative anisotropic scattering (g) values in the visible wavelength range using photonic structures with short-range order. A scattering model is devised based on the structural morphology of samples to explain the wavelength-dependent frequency gap and the g values. We show complete agreement between the experiment and theory, which is supported by the structure factor calculations. Specifically, we find a g value of -0.7 ± 0.2 at the frequency gap in accordance with theoretical calculations. The study puts forward an amenable approach for tailoring the scattering anisotropy values using photonic structure with short-range order and thus mediates an inclination toward the localization.
44.	Skellam Type Processes of Order K and Beyond N Gupta, A Kumar, N Leonenko - Entropy, 2020 **Abstract:** In this article, we introduce the Skellam process of order k and its running average. We also discuss the time-changed Skellam process of order k. In particular, we discuss the space-fractional Skellam process and tempered space-fractional Skellam process via time changes in Skellam process by independent stable subordinator and tempered stable subordinator, respectively. We derive the marginal probabilities, Lévy measures, governing difference-differential equations of the introduced processes. Our results generalize the Skellam process and running average of Poisson process in several directions.
45.	Some measures for fermionic entanglement in the cosmological de Sitter spacetime S Bhattacharya, H Gaur, N Joshi - Physical Review D, 2020 **Abstract:** We investigate two measures of quantum correlations and entanglement, namely the violation of the Bell-Mermin-Klyshko (BMK) inequalities and the quantum discord, for Dirac fermions in the cosmological de Sitter background of dimension four. The BMK violation is focused on the vacuum for two- and four-mode squeezed states and the maximum violation is demonstrated. For the quantum discord, we investigate a maximally entangled in-vacuum state. Qualitative similarities as well as differences of our results with that of different coordinations of de Sitter in the context of scalar and fermionic field theory are discussed.
46.	Spatial Mapping and Feature Analysis for Individual Finger Movements Using High Density Electromyography: Preliminary Study P Mehra, M Dave, A Khan, RKY Tong - Journal of Image and Graphics, 2020 **Abstract:** The analysis between finger movements is an important aspect of biophysics and rehabilitation. The study aims to evaluate the distinctive muscle activities between finger movements through the help of High-Density Electromyographic (EMG) signals for increased myoelectric control of soft robotic hand. 64-channel EMG signal was recorded during individual finger isometric task for 5 healthy subjects. Raw, single differential and double differential EMG signals across the 2D array was analyzed. Spatial image of theses signals for the 4 different finger movement demonstrated multiple distinctive properties, the major distinction. Feature set of six distinct features was calculated for the array of EMG signals to quantitatively differentiation between finger movements. Centroid of these feature set acquired different 3D

	space indicating differences in the finger movements. This indicated that HDEMG could be used for differentiating finger movements and could be used as a method for classification algorithm for increased myoelectric finger control in future.
47.	The Influence of Activities and Socio-Economic/Demographic Factors on the Acceptable Distance in an Indian Scenario TM Rahul, M Manoj, D Tahlyan, A Verma - Transportation in Developing Economies, 2020 **Abstract:** Type of activity is an important aspect that influences the travel behavior of the trip makers. The present study uses the concept of an acceptable trip distance to compare the walking characteristics across subgroups of various socio-demographic factors and the type of activity. It further formulates a multiple linear regression model to investigate the relative influence of various socio-demographic factors and the type of activity on the walking distance; and develops a standalone formula, which reduces the effort of acceptable distance determination, for helping decision-makers to determine the acceptable distance easily. The regression model in the study found that the type of activity had a statistically significant effect on the walking distance. The acceptable distance for the work trips was found to be 996 m and for the 'personal/household business' trips was found to be 263 m. The results of this study were used to devise various policy guidelines including a zonal priority criterion for the development of pedestrian infrastructures and a stratified urban space where individuals would have an option of walking. Further, in the study, the standalone formula for calculating the acceptable distance was determined by equating the third derivative of the theoretical distribution (log-normal) to zero.
48.	Thermal Sensitivity of Dielectric Materials in High-Speed Designs S Pathania, B Mutnury, M Vasa, V Kumar…R Sharma - IEEE 29th Conference on Electrical Performance of Electronic Packaging and Systems (EPEPS), 2020 **Abstract:** At high-speeds, careful analysis is required at the design stage to ensure robust signal integrity (SI) in high-speed printed circuit boards (PCBs). Signal loss in PCBs is predominantly due to conductor loss, dielectric loss and impedance mismatch.In this paper, thermal impact on loss and impedance is studied. In that, thermal sensitivity for standard loss, mid-loss, low-loss and ultra-low loss dielectric materials is studied. It is observed that ultra-low loss materials are less sensitive as compared to standard loss materials. Also, thermal impact on impedance and loss in transmission lines, vias and SMT pads is analyzed.
49.	Wettability of thermoplastic and thermoset polymers with carbon nanotube grafted carbon fiber HS Bedi, S Kumar, PK Agnihotri - Materials Today: Proceedings, 2020 **Abstract:** In this experimental study the wetting behavior of unsized and carbon nanotube (CNT) grafted carbon fibers is assessed with various polymers. Thermoset epoxy and two thermoplastics (polypropylene and polycarbonate) are tested. Sessile drop method and drop-on-fiber method are employed to quantify the wettability of various fiber/polymer combinations. Contact angle measurements based on the above two methods give insights into the effectiveness of various polymers to wet different types of carbon fiber fabrics and single fiber filaments. Moreover, the effect of CNT length and density on the wettability of carbon fibers is ascertained by synthesizing nanotubes on the fiber surface for varying time durations (10–30 min). CNT grafting reduces the contact angle of the polymer drop with carbon fiber; however, too much growth of nanotubes on the fiber surface leads to improper impregnation of the polymer into the carbon fabric. While polypropylene shows better wetting characteristics with unsized and CNT grafted carbon fibers, polycarbonate shows poor wettability.

50.	Workspace Reconstruction for Designing Modular Reconfigurable Manipulators AT Reji, A Dogra, E Singla - Industry 4.0 and Advanced Manufacturing: Part of the Lecture Notes in Mechanical Engineering book series **Abstract:** The world is getting primed for Industry 4.0. In this context, we propose a framework for the automatic reconstruction of workspaces where a manipulator is required to function. The manipulator can be customized using modular and reconfigurable approach with respect to the reconstructed workspace and the set of Task-Space-Locations (TSLs) and Base-Location (BL) specified. Focus is also laid on reducing the size of the workspace model while preserving its geometric features. In essence, our work aims to reduce human intervention in designing manipulators. The framework is developed in Robotic Operating System (ROS). The framework utilizes a depth sensor for generating data from the environment, which undergoes further processing to generate a mesh which represents the workspace. The framework is tested for different workspaces, and the results obtained are discussed.

Disclaimer: This publication digest may not contain all the papers published. Library has compiled the publication data as per the alerts received from Scopus and Google Scholar for the affiliation "Indian Institute of Technology Ropar" for the month of October 2020. The author(s) are requested to share their missing paper(s) details if any, for the inclusion in the next publication digest.